AGU PUBLICATIONS

Geophysical Research Letters

RESEARCH LETTER
10.1002/2016GL068434

Key Points:
- Using a new crater production function for current Mars, the NPLD surface age is closer to ~1.5 kyr
- Accounting for ice target strength suggests that crater model ages are overestimates
- The north polar deposit on Mars is being resurfaced faster than previously calculated

Supporting Information:
- Supporting Information S1
- Table S1

Correspondence to:
M. E. Landis,
mlandis@lpl.arizona.edu

Citation:
Landis, M. E., S. Byrne, I. J. Daubar, K. E. Herkenhoff, and C. M. Dundas (2016), A revised surface age for the North Polar Layered Deposits of Mars, *Geophys. Res. Lett.*, *43*, doi:10.1002/2016GL068434.

Received 25 FEB 2016
Accepted 18 MAR 2016
Accepted article online 23 MAR 2016

A revised surface age for the North Polar Layered Deposits of Mars

Margaret E. Landis[1], Shane Byrne[1], Ingrid J. Daubar[2], Kenneth E. Herkenhoff[3], and Colin M. Dundas[3]

[1]Lunar and Planetary Laboratory, University of Arizona, Tucson, Arizona, USA, [2]Jet Propulsion Laboratory, California Institute of Technology, Pasadena, California, USA, [3]United States Geological Survey, Astrogeology Science Center, Flagstaff, Arizona, USA

Abstract The North Polar Layered Deposits (NPLD) of Mars contain a complex stratigraphy that has been suggested to retain a record of past eccentricity- and obliquity-forced climate changes. The surface accumulation rate in the current climate can be constrained by the crater retention age. We scale NPLD crater diameters to account for icy target strength and compare surface age using a new production function for recent small impacts on Mars to the previously used model of Hartmann (2005). Our results indicate that ice is accumulating in these craters several times faster than previously thought, with a 100 m diameter crater being completely infilled within centuries. Craters appear to have a diameter-dependent lifetime, but the data also permit a complete resurfacing of the NPLD at ~1.5 ka.

1. Introduction

Mars' northern polar deposits are made up of the kilometer thick North Polar Layered Deposits (NPLD), covered by a ~1 m thick residual ice cap (NRIC) and seasonal carbon dioxide frost [*Tanaka et al.*, 2008; *Byrne*, 2009]. The NPLD are composed of layers of water ice with varying dust content, with a bulk dust content of less than 5% based on radar transparency calculations [*Grima et al.*, 2009]. The dust content varies enough to make discrete layers and packets of layers detectable in the Mars Reconnaissance Orbiter (MRO)'s Shallow Radar radargrams [*Phillips et al.*, 2008] and discernable in walls of troughs and scarps. This layering has a postulated link to geologically recent Martian climate change [e.g., *Murray et al.*, 1973; *Thomas et al.*, 1992; *Byrne*, 2009], making the NPLD a key area of research in Mars science.

In order to link these stratigraphic layers to orbital and obliquity cycles, and therefore previous Martian climates, the age and accumulation rate of the NPLD must be understood. The entire NPLD is thought to have accumulated within the last 5 Myr, based on models of ice stability and obliquity-driven climate change [*Jakosky et al.*, 1995; *Laskar et al.*, 2002; *Levrard et al.*, 2007]. Previous work that assigned ages to layers based on accumulation models estimated an average accumulation rate of 0.5 mm yr^{-1} for the top 500 m of the stack [*Hvidberg et al.*, 2012]. Other models suggest the current accumulation rate is variable and may be as high as ~1 mm yr^{-1} [*Fishbaugh and Hvidberg*, 2006; *Levrard et al.*, 2007]. While long-term average accumulation rates are useful in discussing the NPLD as a whole, understanding the current accumulation or ablation rate is important in linking separate layers to previous Martian climates.

The NRIC can be considered the uppermost layer of the NPLD [*Tanaka et al.*, 2008; *Byrne*, 2009]. The present-day accumulation rate on the NRIC can be used to link the well-studied current climate to the past climates recorded in the NPLD. Modeling of ice stability under present-day Mars orbital parameters suggests that the NPLD as a whole should be accumulating ice liberated from reservoirs at the midlatitudes, as northern hemisphere ground ice is expected to have been more extensive in the recent past [*Chamberlain and Boynton*, 2007]. However, ice grain size measurements from the NRIC in late summer suggest that old ice, which has been present long enough for grains to sinter and increase in size, is currently being exposed, and therefore, net ablation is occurring [*Kieffer*, 1990; *Langevin et al.*, 2005]. On the other hand, these same data show that the NRIC is also relatively dust free (maximum dust content at the surface is ~6% [*Langevin et al.*, 2005]), implying that the current surface outside of troughs and scarps has not been exposed long enough for airfall dust to collect (although dust could also be removed by katabatic winds). These lines of evidence are somewhat contradictory, and mass balance may vary spatially and interannually, complicating the picture of the present-day mass balance of the NPLD surface.

In order to constrain the recent history of the NPLD, crater statistics can be used in combination with a crater production function to infer a model surface age or resurfacing rate. Previous studies have estimated a large range of ages based on crater counting on the NRIC. The lack of visible craters larger than 300 m diameter in Viking Orbiter images led *Herkenhoff and Plaut* [2000] to assign a model age of less than 120 ka to the surface. *Tanaka* [2005] concluded that the age of the uppermost layers of the NPLD was 8.7 ± 6.2 ka based on two craters (42 m and 90 m diameter) detected in Mars Orbiter Camera images from Mars Global Surveyor. Most recently, *Banks et al*. [2010] identified 95 craters between 10 and 352 m in diameter in MRO Context Camera (CTX) [*Malin et al*., 2007] images, the diameters of which they measured in High Resolution Imaging Science Experiment (HiRISE) [*McEwen et al*., 2007] and CTX images. Using the *Hartmann* [2005] production function, *Banks et al*. [2010] concluded that the current crater population was in equilibrium. Therefore, crater lifetime was proportional to diameter, and a single model age could not be assigned to the NRIC. They also concluded that the visible craters had all formed within the last ~10–20 kyr.

Here we revisit the work of *Banks et al*. [2010] with a new understanding of the current impact rate on Mars. That previous work used the *Hartmann* [2005] production function, which is based on lunar craters and the radiometric ages of lunar samples. Using a combination of bolide size scaling and corrections for the impact velocities and surface gravities, *Hartmann* [2005] adapted the lunar cratering rate to Mars [see also *Ivanov*, 2001]. However, the production rate of new small (tens of meter diameter) craters on Mars has now been directly measured [*Daubar et al*., 2013], which provides an alternative production function (PF) to compare to the NRIC crater population. This PF represents the current observable small impacting population at Mars. It is relevant over a time scale that is orders of magnitude smaller than that of the *Hartmann* [2005] PF. "Preimpact and postimpact" CTX images record impacts over the past 10 years, rather than the billion-year-old cratering record of the lunar mare. As the *Daubar et al*. [2013] PF is derived from current impacts, any variations in the impactor flux in Mars' recent history (e.g., due to the effects of changing Mars' orbital eccentricity, asteroid breakup, or changes in bolide properties) will be recorded in their present value in the isochrons derived from this PF. Additionally, the *Daubar et al*. [2013] PF does not rely on extrapolation of parameters from the Moon to Mars, which removes several uncertainties such as those in impact velocities, cratering efficiencies, and atmospheric effects. However, this PF has its own uncertainties due to observational biases, including size-dependent differences in lifetimes of blast zones that may result in fewer small (maximum of tens of meter diameter) craters being detected [*Daubar et al*., 2016]. It is also based on observations of craters generally smaller than those on the NRIC and may be subject to more atmospheric and detection bias effects.

In this paper, we reexamine the population of NPLD craters first identified by *Banks et al*. [2010]. We use the new, current PF of impact craters based on impact events currently occurring on the dusty plains of Mars [*Daubar et al*., 2013]. We present results from new HiRISE coverage of craters on the surface of the NPLD previously observed only with CTX [*Banks et al*., 2010]. Combining the revised crater catalog and the new *Daubar et al*. [2013] PF, we reinterpret the history of the current surface of the NPLD.

2. Methods

2.1. Crater Observations

We revise the catalog in *Banks et al*. [2010] by remeasuring crater diameters and locations using a three-point rim measurement technique in HiRISE images using the United States Geological Survey Crater Helper Tools ArcGIS extension. We also acquired HiRISE images of craters identified in only CTX images in the crater catalog of *Banks et al*. [2010]. The region of interest (ROI) (Figure 1) we adopt is the same as the one utilized in *Banks et al*. [2010], which they identified as recently accumulated areas of the NPLD that mostly coincides with the NRIC. *Banks et al*. [2010] selected the ROI (area 7×10^5 km^2) based on three criteria: elevation, surface roughness, and slope. These selection criteria were intended to isolate the dome of Planum Boreum from Chasma Boreale and Vastitas Borealis; to exclude dune fields where crater preservation was unlikely over geologically short time scales; and to eliminate slopes (such as troughs) that receive different amounts of insolation and therefore have an accumulation/ablation rate(s) that differ(s) from the rest of the surface of Planum Boreum [*Smith and Holt*, 2010].

In this ROI, we have 83 impact sites in our catalog (Figure 1 and Table S1), counting each crater or crater cluster as one impact site. The diameters of the craters range from 10 to 360 m. Our catalog cannot be considered

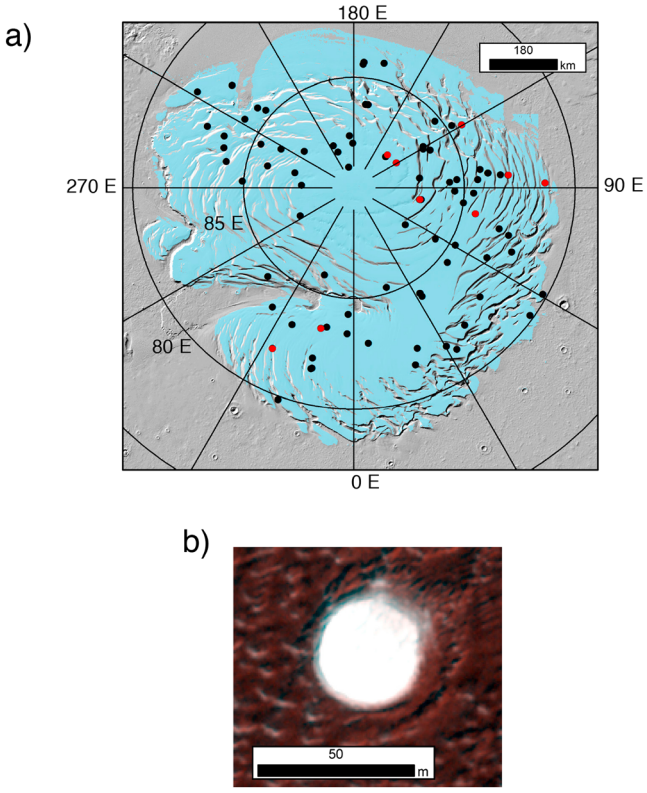

Figure 1. (a) Polar projection map of the NPLD region of interest (blue), locations of craters in our study (black and red), and sites with digitial terrain models (DTMs) (red). The base map is Mars Orbiting Laser Altimeter [*Smith et al.*, 2001] hillshade topography. (b) An example of a crater on the NRIC with interior bright material and defrosted surroundings, (84°N, 237°E in HiRISE image PSP_009223_264). Image: NASA/Jet Propulsion Laboratory/University of Arizona.

to be complete below diameters of ~30 m due to the complex texture of the NRIC at that scale and the 6 m pixel scale of CTX images in which candidate crater sites were initially identified. The lower limit of the smallest diameter bin we consider complete is 31 m, following the convention of *Crater Analysis Techniques Working Group* [1979], where diameter bins start at 1 km diameter and bin edges decrease by a factor of $\sqrt{2}$ with each smaller bin. All 58 impact sites greater than the 31 m diameter cutoff in our catalog now have HiRISE follow-up images.

Two craters (81 m and 30 m diameters) identified in CTX images alone from *Banks et al.* [2010] did not appear in HiRISE follow-up of the same location, likely due to the initial misidentification at CTX's lower resolution. An additional crater site (site 30, 35 m diameter, Table S1) was found in a HiRISE image within the ROI that had not been previously identified. This crater is degraded and was likely overlooked due to the lower resolution of CTX.

Sites of crater clusters that were formed by a single impactor are easily identifiable in this crater population. Each crater in a cluster is within a few hundred meters of the others, whereas the closest crater sites are separated by several kilometers. These crater clusters are not secondary clusters: they do not display the typical herringbone patterns [e.g., *Oberbeck and Morrison* [1973]], they are not present in rays or chains [e.g., *McEwen et al.* [2005]], and there are no nearby large craters that could be the source primary. Primary crater clusters such as these are a significant fraction of new Martian impact detections [*Daubar et al.*, 2013]. In these cases, an effective diameter for the cluster was calculated from the individual crater diameters (D) using the formula: $(\Sigma \cdot D^3)^{(1/3)}$ [*Malin et al.*, 2006; *Ivanov et al.*, 2009]. This scaling approximates the size of the crater that would have formed if the impactor had not broken up in the atmosphere, assuming that the impact events are strength dominated [*Williams et al.*, 2012]. There are eight clusters in our catalog, four of which had an effective diameter above the 31 m lower limit of completeness. This lower limit meets the minimum suggested size of 30 m effective diameter for crater statistics given in *Daubar et al.* [2013].

For craters previously measured in HiRISE images, our diameter measurements were on average 2 ± 5 m different than *Banks et al.* [2010]. This represents at most a 10% difference and is most likely due to subjective determinations of degraded or irregular crater rims. For craters reported in *Banks et al.* [2010] that had only been measured in CTX images, we revise the diameters by a maximum of 23 m (~4 CTX pixels, in this case from a 73 m diameter crater reported in *Banks et al.* [2010] that was remeasured as 50 m in a HiRISE image). Our remeasurements led to eight craters being moved to a smaller diameter bin in the size-frequency distribution (SFD) and two to larger diameter bins.

Using a combination of comparing depth to diameter (d/D) ratios to preservations states as well as statistical arguments (Text S1), we determine that the population of craters on the NRIC is dominated by primary impacts and a viable population for crater age dating.

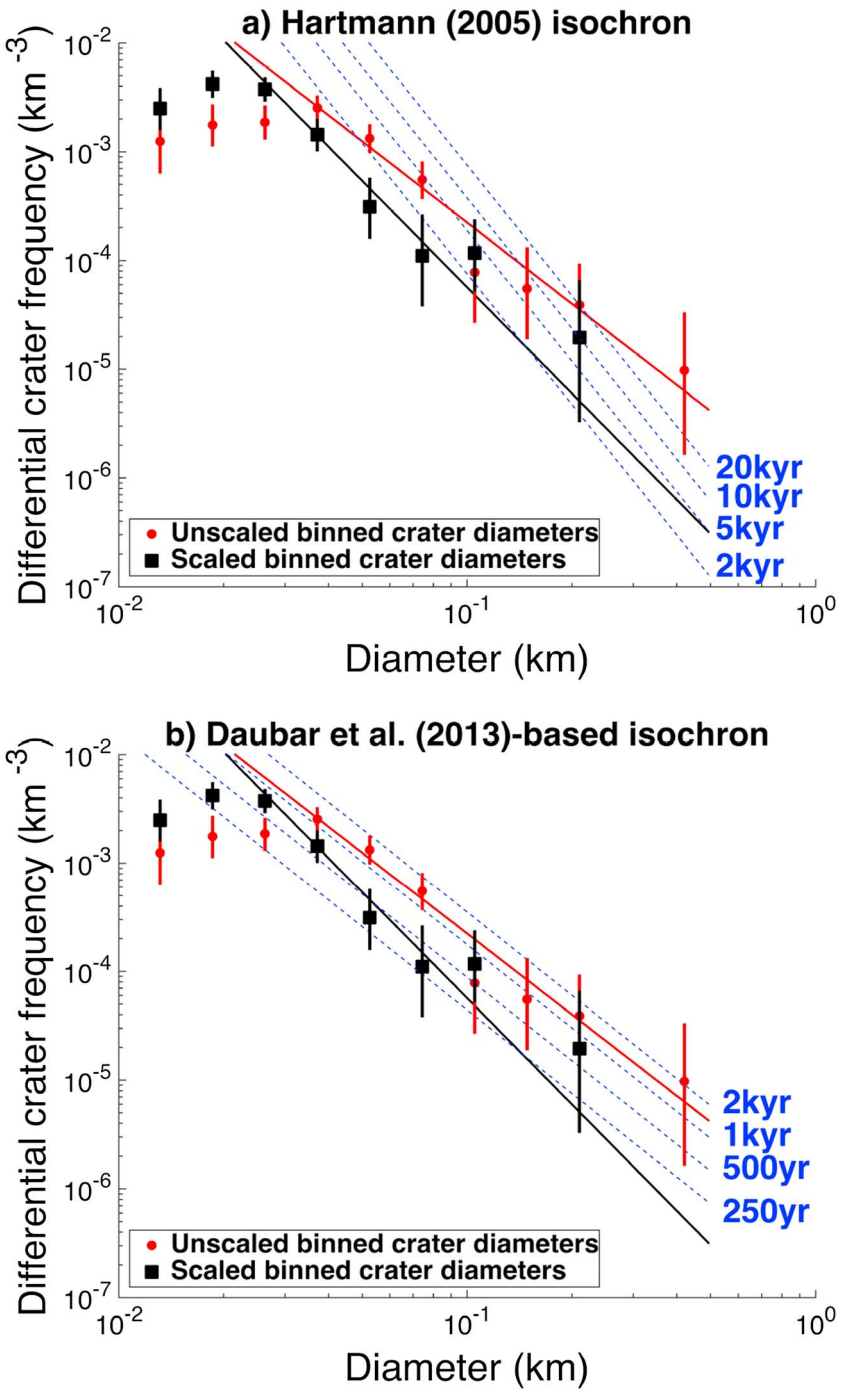

Figure 2. Differential crater size-frequency distribution (SFD) of the NPLD craters plotted with isochrons (dashed blue) from the (a) *Hartmann* [2005]- and (b) *Daubar et al.* [2013]-based PFs. Red points are raw crater data. Black squares are scaled crater diameters, assuming a yield strength of ice of 1 MPa. Solid lines are best fit power laws to the SFDs.

2.2. Crater Statistics

In order to analyze the SFD of the craters, we constructed differential plots according to the conventions of *Crater Analysis Techniques Working Group* [1979]. We deviate from the convention only by using 1 σ errors based on *Gehrels* [1986], which is more appropriate for small number statistics than the usual $\sqrt{N}$ (where N is the number of craters in that bin) for small number statistics. The isochrons generated from the *Daubar et al.* [2013] and *Hartmann* [2005] PF are also plotted (Figure 2). An overall power law fit to the NPLD crater

population was calculated to further explore the statistics of the surface crater population and is presented in section 3.

To calculate the lifetime of craters on the NPLD as a function of crater diameter, we divided the overall differential fit to the crater data (in units of craters km^{-3}) by the PFs (in units of craters $km^{-3}\,yr^{-1}$). This technique was also used in the incremental plots of *Banks et al*. [2010] for calculating the diameter-dependent lifetimes reported there. As both the data and PFs are given as power laws of diameter, the crater lifetimes are also power laws.

One sigma errors were included with the PF calculated from *Daubar et al*. [2013]. To calculate the 1 sigma uncertainties for the crater PF in *Hartmann* [2005], we took the square root of their count in each diameter bin, as *Hartmann* [2005] used the large numbers of craters present on the lunar mare and is not affected by small number statistics. We fit a power law to the numeric values reported in Table 2 in *Hartmann* [2005] using these uncertainties within our diameter range of interest, which yielded a power law production function with 1 sigma uncertainties. Uncertainties in the PFs and the data were then combined to yield uncertainties in the crater lifetimes.

2.3. Strength Scaling and Diameter Correction Factor

The small craters used to derive the PFs of both *Hartmann* [2005] and *Daubar et al*. [2013] formed in regolith, but the impact craters on the NPLD formed in ice-rich material. We used π-group scaling [*Holsapple*, 1993] to calculate a correction factor to be applied to our measured crater diameters, in order to compare them to the PFs. The π-group scaling approach relies on parameters derived from fits to experimental and explosion crater data, and some of these parameters for ice are either estimated or extrapolated from the known values for regolith, bedrock, soft rock, and sand. We took the material at the surface of the NPLD to have the density of water ice [*Holsapple*, 1993], the cohesion parameters of soft rock [*Holsapple*, 1993], zero porosity [*Athern et al*., 2000], and explored effective yield strengths of 0.5 MPa, 1.0 MPa, and 2.0 MPa (which are in the range of effective yield strength of other materials considered in *Holsapple* [1993]). For the regolith target, we used the density, yield strength, and cohesion values for regolith described in *Holsapple* [1993] and *Kite et al*. [2014]. Specific values are listed in a lookup table at http://keith.aa.washington.edu/craterdata/scaling/theory.pdf. We took the ratio of the transient crater diameter in ice to the transient crater diameter in regolith and used it to rescale our measured diameters. By doing this, we assume that these two model craters in different materials collapse to the same extent.

Strength scaling between materials will affect results from the *Daubar et al*. [2013] and the *Hartmann* [2005] PFs equally. Our calculations show that the diameters of transient craters in ice are consistently larger than those in regolith, and therefore, the model ages given by the isochrons from regolith targets will overestimate the age of this icy surface. In addition to raw diameter data, Figure 2 also shows the crater SFD with the correction factor (assuming a yield strength of 1.0 MPa) applied. A noteworthy consequence of this scaling is that the exponent of the fit to the SFD of the corrected diameters differs.

We also considered the effects of viscous relaxation as these small craters are the result of impacts into an ice/dust mixture that flows over sufficiently long time scales. Larger craters ($\gtrsim$1 km diameter) on the South Polar Layered Deposits are affected by viscous relaxation [*Pathare et al*., 2005]. However, a recent study of flow of icy topography of the NPLD using finite element models found that viscous relaxation has been negligible in shaping the topography of presently observed NPLD impact craters [*Sori et al*., 2016]. Therefore, changes in depth are dominated by other factors, like crater infilling.

3. Results

In the results below, we discuss both the unscaled (measured in this paper, Table S1) and scaled (calculated, see section 2.3) diameters of the NPLD craters. We present crater lifetimes as a function of diameter only for the size range included in this study (31 m to 210 m). Extrapolations of crater lifetime beyond this should be regarded with caution. In order to cross compare results, we also discuss an example of the lifetime of a 100 m diameter crater in each case (Table 1).

Table 1. Crater Lifetimes (Years) Are Calculated From the SFD and PF Fits Described in Section 2.2. Diameters (D) Are in Kilometers

	Hartmann [2005]	*Daubar et al.* [2013]
Unscaled crater lifetime	$4.23\times10^{5}D^{1.47\pm0.47}$	$1.48\times10^{3}D^{0.07\pm0.59}$
100 m diameter crater lifetime	14.0 kyr	1.3 kyr
Scaled (1 MPa ice) crater lifetime	$1.84\times10^{4}D^{0.82\pm0.74}$	$64.5\times10^{3}D^{-0.70\pm0.82}$
100 m diameter crater lifetime	2.8 kyr	0.3 kyr

3.1. *Hartmann* [2005] Production Function

Using the *Hartmann* [2005] PF and our measured (unscaled) diameters, we calculate the lifetimes (years) of the individual impact craters (with diameter, D, measured in kilometers) on the NPLD to be

$$4.23\times10^{5}D^{1.47\pm0.47}$$

e.g., the lifetime of a 100 m diameter crater would be ~14 kyr (Table 1). This agrees to within a factor of 2.3 with the *Banks et al.* [2010]-estimated lifetime of ~6 kyr for a 100 m diameter crater. Since the lifetime fit has an exponent that is not equal to zero, the lifetime of craters is diameter dependent; i.e., in this case, the time smaller craters will persist is shorter than for larger craters. The crater population can be interpreted to be in equilibrium, with craters forming and being erased (infilled) as the NPLD accumulate in such a way that the population SFD remains constant. Crater lifetimes are for individual craters of that diameter, and no single age for the surface can be estimated from this.

When crater diameters are adjusted based on strength scaling, the slope of the best fit line to the differential SFD has a larger negative exponent in the power law fit than without the scaling. The scaled best fit line still cuts across isochrons (Figure 2a) and the lifetime function is

$$1.84\times10^{4}D^{0.82\pm0.74}.$$

The overall interpretation with the addition of the strength scaling is still that the NRIC is an equilibrium surface. The model age of a 100 m diameter crater (taking into account target strength scaling) is ~2.8 kyr.

3.2. *Daubar et al.* [2013] Production Function

Using the *Daubar et al.* [2013] PF and unscaled crater diameters, the calculated lifetime of the impact craters becomes

$$1.48\times10^{3}D^{0.07\pm0.59}.$$

A 100 m diameter crater would have a lifetime of ~1.3 kyr, an order of magnitude less than predicted by the *Hartmann* [2005] PF. The exponent of the lifetime fit is 0.07 ± 0.59 (indistinguishable from zero), consistent with the NRIC being an equilibrium or production surface. Craters may be forming and disappearing at a similar rate to produce an equilibrium population. In this case, small and large craters would have the same lifetime, meaning that ice would accumulate faster in the larger (deeper) craters in order for them to disappear as quickly as a small crater. Alternatively, the crater SFD may reflect a production population, where an initially crater-free surface records all impacts from a certain epoch. In this case, the craters would span a range of ages and degradation states and the age of this epoch would be ~1.5 kyr.

When the crater diameter correction from strength scaling is included, the surface age is reduced further by at least a factor of 2 (Figure 2b), i.e., crater lifetime in this case is

$$64.5\ D^{-0.70\pm0.82}$$

(~300 years for a 100 m diameter crater at an effective yield strength of 1.0 MPa). This calculation results in a negative exponent for the crater lifetime, indicating that a 31 m diameter crater (the smallest crater size considered in the statistically complete range) would be preserved longer than a ~200 m diameter crater. There is no physical mechanism that removes larger craters faster than smaller craters, except for viscous relaxation and that has been found to be negligible here [*Sori et al.*, 2016]. The errors on this solution permit a value of zero, and we interpret the actual value to be close to it. This strength-corrected lifetime fit is consistent with a production surface 500 years but more closely matches an equilibrium surface with a weakly diameter-dependent lifetime.

Target strength scaling introduces the largest uncertainty into the interpretation because the π-group scaling yield strength parameter has not been experimentally determined for ice at typical Martian temperatures and was estimated. Scaling from effective yield strengths varying from 0.5 to 2.0 MPa produced exponents on the lifetime calculation from -0.44 ± 0.82 to -0.698 ± 0.42 (corresponding to 100 m diameter crater lifetimes from 280–551 years), translating to another factor of ~2 in uncertainty assuming the minimum 1 sigma uncertainty. We utilize the scaled crater diameters to illustrate that the effect of target strength in lowering the model age of the surface, rather than to suggest that smaller craters have a significantly longer lifetime than larger ones.

4. Discussion

After revisions to the crater catalog of *Banks et al*. [2010], we have calculated the lifetimes of craters on the surface using two separate PFs. Both are expected to be equally affected by diameter scaling effects due to target properties as both PFs were derived from craters in regolith targets.

Due to the different sources of each PF, we consider the results from using the *Daubar et al*. [2013] PF to be more appropriate for the NPLD crater population than those using *Hartmann* [2005]. The diameters of craters considered in the *Hartmann* [2005] PF are based on sizes an order of magnitude larger than the diameters of craters in our ROI, which requires an extrapolation that contributes additional uncertainty. Moreover, the *Hartmann* [2005] system relies on the long baseline of the lunar mare (billion year time scales), many orders of magnitude longer than the relevant time scales for the surface of the NPLD. In contrast, the *Daubar et al*. [2013] PF is based on tens of meter diameter impacts on Mars over the past ten years, and does not include distant secondary craters, and thus, it is our preferred function as it is closer to the NPLD impact population in diameter and time scale.

This opens a new possible interpretation of the recent history of the NPLD. With the *Hartmann* [2005] PF, the crater lifetime is clearly diameter dependent. Using the *Daubar et al*. [2013] PF, the picture becomes less clear. Without the target strength scaling, the fit to the crater SFD suggests a 1.5 kyr old production surface due to diameter independence (to within the uncertainties) of the calculated crater lifetimes. Including target scaling of the crater diameters, the crater lifetimes become weakly diameter dependent, although the uncertainties are large enough that a production surface remains a possibility.

There are two possible ways of generating diameter-independent lifetimes of craters with a model age of ~1.5 kyr. One is that the NPLD have undergone some resurfacing event (accumulation or ablation) that erased all craters on the surface and which would have ended ~1.5 kyr ago. A second scenario is a higher infill rate in larger craters such that they persist only as long as smaller craters. We prefer the resurfacing hypothesis as it is unclear what mechanism would cause infill rates to vary with diameter, as simple crater geometry (and therefore relative length of shadows cast by the rim on the interior and corresponding cold-trapping effect) is size invariant.

Varying accumulation or ablation rates over the ROI is also possible, but the study area was chosen specifically in *Banks et al*. [2010] to remove areas that would clearly undergo different resurfacing rates. Additionally, *Banks et al*. [2010] found no latitude or longitudinal dependence in crater degradation state, suggesting that the ROI does not have large spatial variations in accumulation. Scenarios that could produce an equilibrium surface remain possible and are discussed in depth in *Banks et al*. [2010]. Here we consider the implications of the case in which the NRIC is a production surface caused by a resurfacing event at ~1.5 kyr.

Lack of dust in NRIC ice and exposures of large ice grain sizes [*Langevin et al*., 2005] could be explained by a recent change from net accumulation to net ablation, consistent with a production surface. However, as many of these craters have a $d/D < 0.2$, recent accumulation of ice must be occurring within these craters even if net accumulation is not occurring on adjacent NRIC surfaces. This can be directly observed within the HiRISE images of these craters, e.g., site 33 in (Figure 1b and Table S1), where bright deposits remain within the crater even when the surrounding terrain has defrosted. The interpretation that the NRIC represents a production surface due to a resurfacing event in the recent past is consistent with a recent change in annual mass balance (see section 1).

Mars' orbital elements have not changed significantly in the last several kiloyears [*Laskar et al*., 2004], so any climatic change affecting the NRIC mass balance cannot primarily depend on changes in insolation. The change could be linked to variations in the surface of the south polar residual cap [*Byrne and Ingersoll*,

2003; *Thomas et al*., 2013] on time scales of centuries that could change the atmospheric abundance of water vapor. Variations in albedo (and therefore global temperatures) observed on the surface of Mars due to changes in dust distribution [*Geissler*, 2005; *Fenton et al*., 2007] are also possible. However, *Szwast et al*. [2006] concluded that there was no convincing indication of long-term change in Mars' surface albedo over the most recent decades. Whether these resurfacing and readjustment events are unique to the last ~1.5 kyr on the surface of the NPLD is uncertain and if they did occur are unlikely to be a single event. Most work seeking to interpret NPLD strata relies on insolation history alone. Possible past epochs where net mass balance has changed significantly for as yet unidentified reasons would complicate the interpretation of any stratigraphic record of climate change observed in the NPLD layers.

The PFs of *Daubar et al*. [2013] and *Hartmann* [2005] yield multiple possible interpretations for whether or not the NRIC reflects a production or equilibrium surface. The two PFs also produce an order of magnitude difference in derived ages and therefore in the intracrater ice accumulation rates. Future modeling of ice accumulation rates within and around these craters will be needed to distinguish between these possible recent scenarios of NPLD history.

Acknowledgments

This work was funded by NASA grant NNX13AG72G. M.E.L. was supported by the National Science Foundation Graduate Research Fellowship Program, grant DGE-1143953. HiRISE images referenced are available on the instrument's public website: https://hirise.lpl.arizona.edu. The crater catalog used in this work is included with this paper as supporting information. The authors thank S. Sutton for help with SOCET Set software, M.M. Sori for useful discussion on viscous relaxation, and M.E. Banks for useful discussion on the impact population. The authors additionally thank J. A. Skinner, P. Becerra, D. Laikko, M. Sori, N. Barlow, and an anonymous reviewer for helpful comments on the manuscript.

References

Athern, R. J., D. P. Winebrenner, and E. D. Waddington (2000), Densification of water ice deposits on the residual north polar cap of Mars, *Icarus*, *144*(2), 367–381, doi:10.1006/icar.1999.6308.

Banks, M. E., S. Byrne, K. Galla, A. S. McEwen, V. J. Bray, C. M. Dundas, K. E. Fishbaugh, K. E. Herkenhoff, and B. C. Murray (2010), Crater population and resurfacing of the Martian north polar layered deposits, *J. Geophys. Res.*, *115*, E08006, doi:10.1029/2009JE003523.

Byrne, S. (2009), The polar deposits of Mars, *Annu. Rev. Earth Planet. Sci.*, *37*, 535–360, doi:10.1146/annurev.earth.031208.100101.

Byrne S., A. P. Ingersoll (2003), Martian climatic events on timescales of centuries: Evidence from feature morphology in the residual south polar ice cap, *Geophys. Res. Lett.*, *30*(13), 1696, doi:10.1029/2003GL017597.

Chamberlain, M. A., and W. V. Boynton (2007), Response of Martian ground ice to orbit-induced climate change, *J. Geophys. Res.*, *112*, E06009, doi:10.1029/2006JE002801.

Crater Analysis Techniques Working Group (1979), Standard techniques for presentation and analysis of crater size-frequency data, *Icarus*, *37*(2), 467–474, doi:10.1016/0019-1035(79)90009-5.

Daubar, I. J., A. S. McEwen, S. Byrne, M. R. Kennedy, and B. Ivanov (2013), The current Martian cratering rate, *Icarus*, *225*(1), 506–516, doi:10.1016/j.icarus.2013.04.009.

Daubar, I. J., C. M. Dundas, S. Byrne, P. Geissler, G. D. Bart, A. S. McEwen, P. S. Russell, M. Chojnacki, and M. P. Golombek (2016), Changes in blast zone albedo patterns around new Martian impact craters, *Icarus*, *267*, 86–105, doi:10.1016/j.icarus.2015.11.032.

Fenton, L. K., P. E. Geissler, and R. M. Haberle (2007), Global warming and climate forcing by recent albedo changes on Mars, *Nature*, *446*, 646–649, doi:10.1038/nature05718.

Fishbaugh, K. E., and C. S. Hvidberg (2006), Martian north polar layered deposits stratigraphy: Implications for accumulation rates and flow, *J. Geophys. Res.*, *111*, E06012, doi:10.1029/2005JE002571.

Gehrels, N. (1986), Confidence limits for small numbers of events in astrophysical data, *Astrophys. J.*, *303*, 336–346, doi:10.1086/164079.

Geissler, P. E. (2005), Three decades of Martian surface changes, *J. Geophys. Res.*, *110*, E02001, doi:10.1029/2004JE002345.

Grima, C., W. Kofman, J. Mouginot, R. J. Phillips, A. Herique, D. Biccari, R. Seu, and M. Cutigni (2009), North polar layered deposits of Mars: Extreme purity of the water ice, *Geophys. Res. Lett.*, *36*, L03203, doi:10.1029/2008GL036326.

Hartmann, W. K. (2005), Martian cratering 8: Isochron refinement and the chronology of Mars, *Icarus*, *174*(2), 294–320, doi:10.1016/j.icarus.2004.11.023.

Herkenhoff, K. E., and J. J. Plaut (2000), Surface ages and resurfacing rates of the polar layered deposits on Mars, *Icarus*, *144*(2), 243–253, doi:10.1006/icar.1999.6287.

Holsapple, K. A. (1993), The scaling of impact processes in planetary sciences, *Annu. Rev. Earth Planet. Sci.*, *21*, 333–373, doi:10.1146/annurev.ea.21.050193.002001.

Hvidberg, C. S., K. E. Fishbaugh, M. Winstrup, A. Svensson, S. Byrne, and K. E. Herkenhoff (2012), Reading the climate record of the Martian polar layered deposits, *Icarus*, *221*, 405–419, doi:10.1016/j.icarus.2012.08.009.

Ivanov, B. A. (2001), Mars/Moon cratering rate ratio estimates, *Space Sci. Rev.*, *96*, 87–104.

Ivanov, B. A., H. J. Melosh, A. S. McEwen, and HiRISE Team (2009), Small impact crater clusters in high resolution HiRISE images—II. Lunar Planet. Sci. 40. Abstract 1410.

Jakosky, B. M., B. G. Henderson, and M. T. Mellon (1995), Chaotic obliquity and the nature of the Martian climate, *J. Geophys. Res.*, *100*, 1579–1584, doi:10.1029/94JE02801.

Kieffer, H. H. (1990), H_2O grain size and the amount of dust in Mars' residual north polar cap, *J. Geophys. Res.*, *95*(B2), 1481–1493, doi:10.1029/JB095iB02p01481.

Kite, E. S., J.-P. Williams, A. Lucas, and O. Aharonson (2014), Low paleopressure of the Martian atmosphere estimated from the size distribution of ancient craters, *Nat. Geosci.*, *7*, 335–339, doi:10.1038/ngeo2137.

Langevin, Y., F. Poulet, J.-P. Bibring, B. Schmitt, S. Douté, and B. Gondet (2005), Summer evolution of the north polar cap of Mars as observed by OMEGA/Mars express, *Science*, *307*, 1581–1584, doi:10.1126/science.1109438.

Laskar, J., B. Levrard, and J. F. Mustard (2002), Orbital forcing of the Martian polar layered deposits, *Nature*, *419*, 375–377, doi:10.1038/nature01066.

Laskar, J., A. C. M. Correia, M. Gastineau, F. Joutel, B. Levrard, and R. Robutel (2004), Long term evolution and chaotic diffusion of the insolation quantities of Mars, *Icarus*, *170*, 343–64, doi:10.1016/j.icarus.2004.04.005.

Levrard, B., F. Forget, F. Montmessin, and J. Laskar (2007), Recent formation and evolution of northern Martian polar layered deposits as inferred from a Global Climate Model, *J. Geophys. Res.*, *112*, E06012, doi:10.1029/2006JE002772.

Malin, M. C., K. S. Edgett, L. V. Posiolova, S. M. McColley, and E. Z. Noe Dobrea (2006), Present-day impact cratering rate and contemporary gully activity on Mars, *Science*, doi:10.1126/science.1135156.

Malin, M. C., et al. (2007), Context camera investigation on board the Mars Reconnaissance Orbiter, *J. Geophys. Res.*, *112*, EOSSO4, doi:10.1029/2006JE002808.
McEwen, A. S., B. S. Preblich, E. P. Turtle, N. A. Artemieva, M. P. Golombek, M. Hurst, R. L. Kirk, D. M. Burr, and P. R. Christensen (2005), The rayed crater Zunil and interpretations of small impact craters on Mars, *Icarus*, *176*, 351–381, doi:10.1016/j.icarus.2005.02.009.
McEwen, A. S., et al. (2007), Mars Reconaissance Orbiter's High Resolution Imaging Science Experiment (HiRISE), *J. Geophys. Res.*, *112*, E05S02, doi:10.1029/2005JE002605.
Murray, B. C., W. R. Ward, and S. C. Yeung (1973), Periodic insolation variations on Mars, *Science*, *180*, 368–640, doi:10.1126/science.180.4086.638.
Oberbeck, V. R., and R. H. Morrison (1973), On the formation of lunar herring-bone pattern, Lunar Planet. Sci. IV, 107–123.
Pathare, A. V., D. A. Paige, and E. Turtle (2005), Viscous relaxation of craters within the Martian south polar layered deposits, *Icarus*, *174*, 396–418, doi:10.1016/j.icarus.2004.10.031.
Phillips, R. J., et al. (2008), Mars north polar deposits: Stratigraphy, Age, and geodynamical response, *Science*, *320*, 1182–1185, doi:10.1126/science.1157546.
Smith, D. E., et al. (2001), Mars Orbiter Laser Altimeter: Experiment summary after the first year of global mapping of Mars, *J. Geophys. Res.*, *106*, 23,689–23,722, doi:10.1029/2000JE001364.
Smith, I. B., and J. W. Holt (2010), Onset and migration of spiral troughs on Mars revealed by orbital radar, *Nature*, *465*, 450–453.
Sori, M. M., S. Byrne, C. W. Hamilton, and M. E. Landis (2016), Viscous flow rates of icy topography on the north polar layered deposits of Mars, *Geophys. Res. Lett.*, *43*, 541–549, doi:10.1002/2015GL067298.
Szwast, M. A., M. I. Richardson, and A. R. Vasavada (2006), Surface dust redistribution on Mars as observed by the Mars Global Surveyor and Viking orbiters, *J. Geophys. Res.*, *111*, E11008, doi:10.1029/2005JE002485.
Tanaka, K. L. (2005), Geology and insolation-driven climatic history of Amazonian north polar materials on Mars, *Nature*, *437*, 991–994, doi:10.1038/nature04065.
Tanaka, K. L., J. A. P. Rodriguez, J. A. Skinner, M. C. Bourke, C. M. Fortezzo, K. E. Herkenhoff, E. J. Kolb, and C. H. Okubo (2008), North polar region of Mars: Advances in stratigraphy, structure, and erosional modification, *Icarus*, *196*, 318–358, doi:10.1016/j.icarus.2008.01.021.
Thomas, P. C., W. M. Calvin, P. Gierasch, R. Haberle, P. B. James, and S. Sholes (2013), Time scales of erosion and deposition recorded in the residual south polar cap of Mars, *Icarus*, *225*, 923–932.
Thomas, P., S. Squyres, K. Herkenhoff, A. Howard, and B. Murray (1992), Polar deposits of Mars, in *Mars*, vol. 23, edited by H. H. Kieffer et al., pp. 767–795, Univ. Ariz. Press, Tucson.
Williams, J.-P., A. Pathare, and O. Aharonson (2012), Modeling small impact crater populations on Mars Euro. Planet. Sci. Congr., 7, 95, (abstract).